



Direct visualization of protein interactions in plant cells

Rajagopal Subramaniam^{1,2†}, Darrell Desveaux^{1†}, Catherine Spickler¹, Stephen W. Michnick¹, and Normand Brisson^{1*}

The protein NPR1/NIM1 is required for the induction of systemic acquired resistance (SAR) in plants and has been shown to interact with members of the TGA/OBF family of basic leucine zipper (bZIP) transcription factors. However, to date, there is no method available to monitor such interactions in plant cells. We report here an *in vivo* protein fragment complementation assay (PCA), based on association of reconstituted murine dihydrofolate reductase (mDHFR) with a fluorescent probe to detect protein–protein interaction *in planta*. We demonstrate that the interaction between *Arabidopsis* NPR1/NIM1 and the bZIP factor TGA2 is induced by the regulators of SAR, salicylic acid (SA), and its analog 2,6-dichloroisonicotinic acid (INA) with distinct species-specific responses. Furthermore, the induced interaction is localized predominantly in the nucleus. Protein fragment complementation assays could be of value to agricultural research by providing a system for high-throughput biochemical pathway mapping and for screening of small molecules that modulate protein interactions.

Systemic acquired resistance is an important disease resistance mechanism that leads to broad-based resistance in noninfected, secondary plant tissues¹. It is characterized by the activation of pathogenesis-related (PR) genes and the accumulation of PR proteins, many of which exhibit antimicrobial activity. Induction of SAR is preceded by an increase in the level of SA, an endogenous signaling molecule^{2,3}. In addition to pathogen infection, SAR can be induced in many plant species by the application of SA or two synthetic analogs, INA and benzothiadiazole^{4,5}.

In *Arabidopsis*, genetic analysis has revealed that the NPR1 protein (also known as NIM1) is required for SAR induction and acts downstream from SA in the SAR pathway. *npr1* mutant plants fail to express several PR genes and show enhanced susceptibility to infection. NPR1/NIM1 was cloned recently and shown to encode a novel protein containing ankyrin repeats^{6,7}. NPR1/NIM1 shares limited sequence similarity with Iκ-Bα (ref. 7), which in mammals binds to and controls the activity of NF-κB, a transcription factor involved in the control of the innate immune system. Yeast two-hybrid experiments revealed that NPR1/NIM1 interacts with members of the TGA family of bZIP transcription factors^{8–10}. Some of these factors, such as TGA2 and TGA3, have been shown to bind to SA-responsive promoter elements of *PR1*, a PR gene induced during SAR, suggesting that NPR1/NIM1 and these two TGA factors act coordinately to regulate expression of SAR genes^{9,10}. Recently, it has been demonstrated that nuclear localization of NPR1/NIM1 is required for its ability to induce *PR1* expression¹¹. These studies suggest a model where, on stimulation of the SAR pathway by SA, NPR1/NIM1 is activated and able to interact, presumably in the nucleus, with a subset of the TGA factors, leading to activation of SAR genes.

To test this model, we developed a method to directly visualize protein interactions in plant cells. This method is based on an *in vivo* protein fragment complementation assay that relies on protein interaction-induced folding of murine dihydrofolate reductase fragments^{12–14}. The basis of this assay (Fig. 1) is that complemen-

tary fragments of DHFR, when fused to interacting proteins and expressed in cells, will fold and reassemble into the complete three-dimensional structure of the enzyme. The reconstituted enzyme is able to bind fluorescein-conjugated methotrexate (fMTX), a high-affinity ($K_d = 540$ pM) inhibitor of DHFR, in a 1:1 complex. Unbound fMTX is actively transported out of the cells¹⁴, whereas fMTX–DHFR complexes are retained in cells and can be monitored by spectroscopy, fluorescence-activated cell sorting (FACS), or fluorescence microscopy. The PCA strategy provides for a direct and quantitative functional analysis of induced or constitutive protein–protein interactions. Genes are expressed in the relevant cell type, and the resulting proteins reflect the native biological state, including correct post-translational modifications. Protein function can be assessed in the appropriate subcellular context, and direct, simple, and unambiguous visualization of the locations of protein complexes can be made. This strategy has been demonstrated to allow for quantitative detection of protein–protein interactions among protein pairs and of allosteric transitions in membrane-associated receptors in living mammalian cells. Furthermore, dose dependence was demonstrated to be consistent with the known pharmacological responses for induced protein–protein interactions^{13,14}.

Other techniques to detect protein–protein interactions have been developed in mammalian systems. Fluorescence resonance energy transfer strategies should, in principle, produce results similar to the PCA in plants, provided adequate control of matched expression levels of proteins can be achieved^{15,16}. A β-galactosidase subunit complementation strategy also could provide information about protein interactions, but background signal due to spontaneous subunit assembly is high, and cells thus must be selected for low expression of fusion proteins¹⁷. Furthermore, plants exhibit a high level of intrinsic β-galactosidase activity, limiting the applicability of this assay to plant cells¹⁸. Finally, immunofluorochemical techniques could complement PCA, but results would reveal only colocalization of proteins.

¹Department of Biochemistry, Université de Montréal, Montréal, Canada H3C 3J7. ²Current address: Department of Biology, University of North Carolina, Chapel Hill. *Corresponding author (normand.brisson@umontreal.ca). [†]These authors contributed equally to this work.

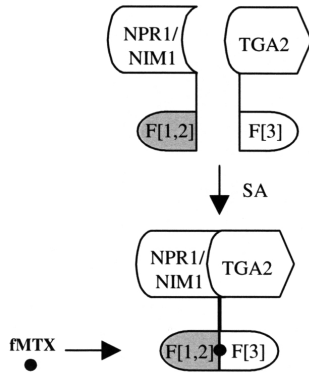


Figure 1. Experimental approach to study interactions between NPR1/NIM1 and TGA2 by PCA in plant cells. Two complementary fragments of murine DHFR are fused to the C terminus of *NPR1/NIM1* and *TGA2*, and the fusion proteins are expressed in plant protoplasts. The interaction between NPR1/NIM1 and TGA2, which facilitates the folding/reassembly of the two DHFR fragments, is monitored by the binding of fMTX to the reconstituted DHFR enzyme.

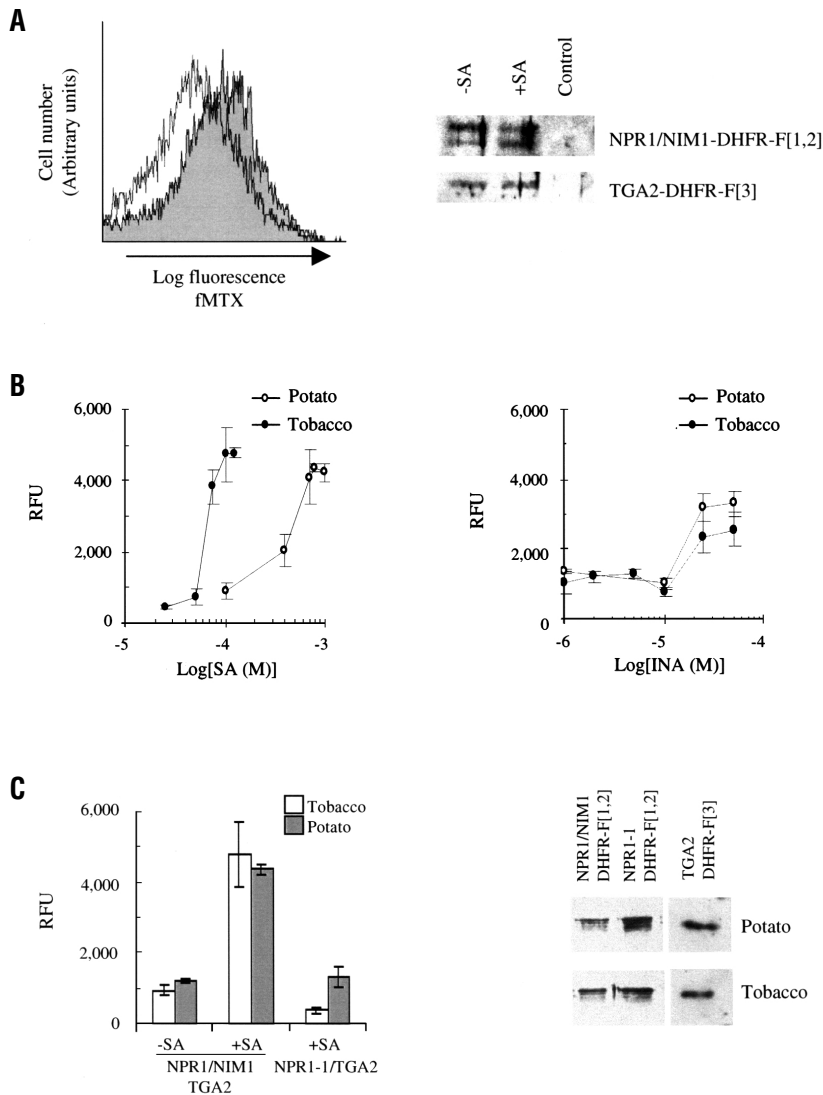


Figure 2. Salicylic acid and INA induce the interaction between NPR1/NIM1 and TGA2 in tobacco and potato. (A) Plant protoplasts expressing NPR1/NIM1 and TGA2–DHFR fusion proteins show increased fluorescence as measured by FACS analysis. In the presence of SA, tobacco protoplasts electroporated with *NPR1/NIM1–DHFR-F[1,2]* and *TGA2–DHFR-F[3]* fusion genes exhibited an increased mean cell population fluorescence (shaded) as compared with untreated protoplasts (line). Western blot analysis with anti-DHFR antibodies shows that SA treatment does not alter the expression levels of either NPR1/NIM1 or TGA2 proteins in these protoplasts. (B) The SA- and INA-induced interaction between NPR1/NIM1 and TGA2 is dosage dependent in tobacco and potato. Protoplasts were treated with the indicated concentrations of SA and INA, and the interaction was quantified by fluorescence spectroscopy. The points represent values of triplicates with standard error. (C) The SA-induced interaction between NPR1/NIM1 and TGA2 is specific. Protoplasts were coelectroporated with *TGA2–DHFR-F[3]* and either wild-type *NPR1/NIM1–DHFR-F[1,2]* or the mutant *NPR1-1–DHFR-F[1,2]* fusion genes and treated with 150 μ M (tobacco) or 700 μ M (potato) SA, and the interaction was quantified by fluorescence spectroscopy. The points represent values of triplicates with standard error. The expression levels of NPR1/NIM1, NPR1-1, and TGA2 fusion proteins were monitored by western blot analysis using anti-DHFR antibodies. Control represents protein extracted from protoplasts that were not electroporated with DNA. RFU, relative fluorescence units.

Results and Discussion

The fluorescence response of tobacco protoplasts co-transformed with *NPR1/NIM1–DHFR-F[1,2]* and *TGA2–DHFR-F[3]* was first quantified by FACS. The SA-induced formation of NPR1/TGA2 complex was monitored by the shift in mean cell population fluorescence in SA-treated as compared with untreated protoplasts. The shift in fluorescence (Fig. 2A) observed indicates that NPR1/NIM1 and TGA2 interact *in planta* and that this interaction is induced by SA. The treatment with SA does not alter overall amounts of the NPR1/NIM1 or TGA2 fusion proteins. However, there is a stoichiometric change between the two bands of the NPR1/NIM1 protein that may be the result of post-translational modification (Fig. 2A). The interaction was characterized further in tobacco by performing a dose–response analysis of SA. Tobacco protoplasts exhibited enhanced fluorescence intensity in response to increasing SA concentrations, with an effective concentration (EC_{50}) of 69 μ M SA (Fig. 2B). The induced response to SA reached its maximum value over a very narrow concentration range (Hill exponent of 8.6). A similar response was observed in potato protoplasts; however, much higher levels of SA were required to induce the interaction (EC_{50} of 590 μ M). As observed with tobacco protoplasts, maximum response in potato also was observed over a narrow concentration range of SA (Hill exponent of 6.5) (Fig. 2B). In both cases, the

large Hill exponent suggests that the interaction between NPR1/NIM1 and TGA2 is the result of a sensitive signaling cascade in which the cooperative response amplifies the signal from upstream or is the result of positive feedback from downstream events¹⁹. This may be important in the stringent regulation of various signal transduction pathways involving NPR1/NIM1 or TGA2. The higher level of SA required to induce the interaction in potato may reflect a more active mechanism of SA detoxification, such as that provided by the SA-inducible UDP-glucose SA glucosyltransferase²⁰. The resulting SA glucoside does not activate SAR but has been

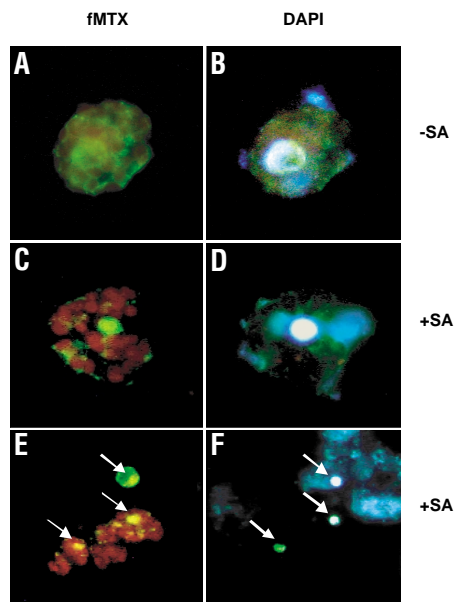


Figure 3. The SA-induced interaction between NPR1/NIM1 and TGA2 is located in the nucleus. (A–F) Potato protoplasts electroporated with *NPR1/NIM1-DHFR-F[1,2]* and *TGA2-DHFR-F[3]* were examined by fluorescence microscopy. Individual protoplasts (A–D) and a group of protoplasts (E, F) were visualized using a fluorescein filter (excitation 460 ± 10 nm and emission 520 ± 10 nm) to detect fluorescence due to fMTX (A, C, E) or a UV filter (excitation 365 nm and emission 420 nm) to detect DAPI staining (B, D, F). (A, B) protoplasts not treated with SA. (C–F) Protoplasts treated with $700 \mu\text{M}$ SA. Arrows in E and F indicate nuclei. On average, 60% of electroporated protoplasts treated with SA showed nuclear localized fluorescence. Magnification: A–D, $\times 100$; E, F, $\times 40$.

proposed to serve as a slow-release storage pool for SA. A constitutive level of fluorescence was observed in both potato and tobacco protoplasts in the absence of exogenous SA. This may be the result of activation of the NPR1/NIM1 pathway during protoplast isolation and electroporation because these processes are known to induce defense-related genes²¹. Nevertheless, the possibility that NPR1/NIM1 can interact with TGA2 in the absence of any inducer cannot be ruled out.

2,6-Dichloroisonicotinic acid has been shown to induce the same set of defense response genes as SA in many plants and therefore behaves as a functional analog of SA. Furthermore, genetic evidence indicates that INA action requires a functional *NPR1/NIM1* gene²². Like SA, INA also induced the interaction of NPR1/NIM1 with TGA2 (Fig. 2B), confirming that the interaction detected in our system is relevant to the function of NPR1/NIM1 in plants. In contrast with SA, the INA-induced interaction occurred at similar EC_{50} values both in tobacco and potato ($23.5 \mu\text{M}$ and $22.5 \mu\text{M}$, respectively), suggesting that the difference in SA-effective concentrations observed between these species indeed might be because of an SA-specific detoxification mechanism and not fundamental differences in signal transduction pathways between the two plant species. The EC_{50} values for INA were much lower than those measured for SA, which is consistent with the lower concentrations of INA required to induce SAR when directly applied to plants²³. However, the maximum level of interaction induced by INA was lower than that induced by SA, suggesting that SA could activate additional signaling pathways that affect the NPR1/NIM1–TGA2 interaction. Alternatively, INA could be a less efficient activator of the SA-induced NPR1/NIM1 pathway.

The correlation of loss-of-function mutations with loss of interaction is a powerful way to directly demonstrate the biological relevance of potential interactions. We therefore tested the ability of NPR1-1 protein to interact with TGA2. NPR1-1 contains a histidine-

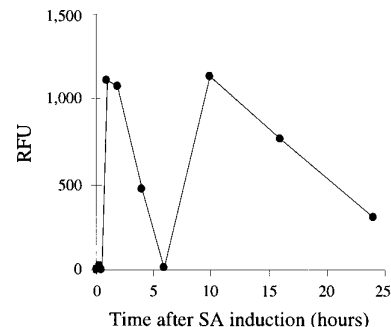


Figure 4. The NPR1/NIM1–TGA2 interaction shows a biphasic temporal pattern in response to SA treatment. Tobacco protoplasts electroporated with *NPR1/NIM1-DHFR-F[1,2]* and *TGA2-DHFR-F[3]* were incubated 10 h in the dark followed by a 10 h treatment with fMTX before treatment with $150 \mu\text{M}$ SA. Fluorescence was measured by fluorescence spectroscopy in the absence of SA and 0.25, 0.5, 1, 2, 4, 6, 10, 16, and 24 h after SA treatment. Points indicate the increase in fluorescence due to the presence of SA and are representative of three independent experiments. RFU, relative fluorescence units.

to-tyrosine replacement in one ankyrin-like repeat at position 334, and *npr1-1* plants are unable to mount a SAR²³. As demonstrated (Fig. 2C), SA did not induce the interaction between NPR1-1 and TGA2, although both proteins were expressed at similar levels (Fig. 2C). These results confirm that the interaction between NPR1/NIM1 and TGA2 observed by the PCA is specific and relevant to the biological function of NPR1/NIM1.

NPR1/NIM1 is localized in both the cytoplasm and the nucleus of unstimulated tissue⁹ and accumulates in the nucleus in response to SA treatment¹¹. The formation of a fMTX–NPR1/NIM1–TGA2 complex permitted us to determine the location of the interaction on SA treatment by fluorescence microscopy. Before SA treatment, fluorescence was dispersed evenly throughout the electroporated protoplasts (Fig. 3A). However, after SA treatment, fluorescence was localized mostly in one region of the cell (Fig. 3C, E). Staining with 4,6-diamidino-2-phenylindole (DAPI) (Fig. 3D, F) revealed that the observed fluorescence (Fig. 3C, E) was in the nucleus, thus indicating that the interaction between NPR1/NIM1 and TGA2 occurs predominantly in this cell compartment after SA treatment. Therefore, we would propose that in response to SA, NPR1/NIM1 interacts with TGA2 and possibly with other TGA factors in the nucleus, leading to activation of genes required for the establishment of SAR (ref. 9).

To examine the temporal pattern of the NPR1/NIM1–TGA2 interaction in response to SA, we measured fluorescence at various time points after addition of SA (Fig. 4). We allowed a 10 h expression period after electroporation to allow the accumulation of the interacting proteins before addition of fMTX and SA. The NPR1/NIM1–TGA2 interaction shows a biphasic mode of interaction in response to SA treatment (Fig. 4), with an early response peaking at roughly 1–2 h and a delayed response at ~ 10 h. Interestingly, pathogen infection has been shown to induce a biphasic accumulation of active oxygen species, which is followed by a similar pattern of SA accumulation and expression of defense-related genes, including *PR1* (refs. 24, 25). Therefore, the biphasic pattern of NPR1/NIM1–TGA2 interaction observed supports the hypothesis that this interaction mediates the expression of *PR1*.

Further investigation using the strategies described here will help determine the biological relevance of other proteins involved in SA-induced SAR as well as other biochemical pathways in plants. It also should be possible to develop a PCA to study protein–protein interactions in whole plant tissues. In summary, our results demonstrate that with the PCA technique, it is possible to visualize an inter-



action in its true context and investigate how the interaction is regulated, as has been demonstrated in mammalian cells²⁶. In addition, the technique will allow the identification of novel interactions and the functional annotation of plant genomes.

Experimental protocol

DNA constructs. Plasmid pBI223D was used to prepare the fusion constructs. This plasmid contains a double 35S enhancer element of the cauliflower mosaic virus (CaMV) and was created by replacing the single 35S enhancer element from the vector pBI221 (Clontech, Palo Alto, CA). The complementary DNAs *NPR1/NIM1* and *TGA2* from *Arabidopsis* were amplified by PCR with *NotI* and *Clal* linkers at the 5' and 3' ends of the genes, respectively. *NPR1-1* was created from the *NPR1* clone by using the ExSite PCR-based site-directed mutagenesis kit (Stratagene, La Jolla, CA). The complementary murine DHFR fragments F[1,2] and F[3] were isolated from the plasmid pMT3 (ref. 12) and inserted into pBI223D. The DHFR fragment F[1,2] was cloned as a C-terminal fusion to *NPR1/NIM1* and *NPR1-1* genes, respectively, and the DHFR F[3] fragment was cloned as a C-terminal fusion to the *TGA2* gene. All the plasmid constructs were verified by sequencing.

Protoplast preparation and electroporation. Leaf mesophyll protoplasts were isolated from six-week-old *in vitro* grown potato plants cv. Kennebec and four-week-old tobacco plants cv. Xanthi as described²¹, except that the enzymatic solution contained 0.8% wt/vol cellulysin and 0.1% wt/vol macerage. We conducted electroporation of protoplasts with a homemade capacitor discharge system, using the disposable electroporation chambers (0.4 cm) of the Cell-Porator System (Gibco-BRL, Gaithersburg, MD). The electrical pulse was delivered from a 1,000 μ F capacitor charged at 125 V for potato and 250 V for tobacco, respectively. Pulses from the electroporator were delivered to 320 μ l of protoplasts (600,000/ml) to which was added 80 μ l of a solution containing 20 mM HEPES, 300 mM NaCl, 10 mM CaCl₂, 770 mM mannitol, and 15 μ g of supercoiled plasmid DNA and 10 μ g of the plasmid pBI221. This plasmid contains the *Escherichia coli uidA* gene, encoding the β -glucuronidase (GUS) enzyme, under the control of the CaMV 35S promoter and was used to correct for variations in electroporation efficiency. All the plasmids were prepared by Qiagen endofree DNA Maxi kits (Qiagen, Chatsworth, CA). After electroporation and a subsequent recovery period of 45 min, 10 μ M fMTX (Molecular Probes, Eugene, OR) along with appropriate concentrations of SA was added to the protoplasts and incubated in the dark for 18 h at room temperature. The protoplasts were washed three times in culture media with an incubation of 30 min at 37°C between washes.

Fluorescence-activated cell sorting analysis. The treated protoplasts were resuspended in 750 μ l of solution containing 154 mM NaCl, 125 mM CaCl₂, 5 mM KCl, and 5 mM glucose (pH 7.9) for FACS analysis. Histograms are based on analysis of fluorescence intensity for 10,000 cells at flow rates of 500–1,000 events per second. Data were collected on a FACSCaliber (Becton-Dickinson, Franklin Lakes, NJ) FACS analyzer with stimulation with an argon tuned to 488 nm with emission recorded through a 530 \pm 15 nm band width filter.

Spectrofluorometry analysis. At each concentration of SA and INA, protoplasts were electroporated with 10 μ g of pBI221 and either 15 μ g of *NPR1/NIM1-DHFR-F[1,2]* alone or 15 μ g each of *NPR1/NIM1-DHFR-F[1,2]* and *TGA2-DHFR-F[3]* fusion constructs. The final concentration of DNA for each electroporation was 40 μ g. In the case in which only the *NPR1/NIM1-DHFR-F[1,2]* was electroporated, 15 μ g of pBI223D plasmid DNA was added. Aliquots were set aside for measuring GUS activity²¹. The protoplasts were processed as before and lysed in 600 μ l 100 mM sodium phosphate buffer (pH 7.9). After centrifugation, 200 μ l of supernatant was aliquoted into a 96-well microtiter plate for fluorometer reading using the Packard Fluorocount fluorometer (excitation 485 nm and emission at 530 nm). The relative fluorescence units were obtained by subtracting the fluorescence values (corrected for GUS activity and protein content) of protoplasts expressing the single construct *NPR1/NIM1-DHFR-F[1,2]* from the fluorescence values of protoplasts expressing both *NPR1/NIM1-DHFR-F[1,2]* and *TGA2-DHFR-F[3]* fusion constructs at each SA and INA concentration.

Fluorescence microscopy. Potato protoplasts were electroporated with *NPR1/NIM1-DHFR-F[1,2]* and *TGA2-DHFR-F[3]* and processed as before, except that after the second wash in the culture media, protoplasts were incubated in DAPI nucleic acid stain at a final concentration of 1 μ g/ml in culture medium for 30 min. Protoplasts were washed once with the culture medium and examined by fluorescence microscopy. We performed microscopy with a Zeiss Axioskop microscope and selective filters.

Acknowledgments

We are very grateful to Dr. Pierre Fobert, National Research Council of Canada, Saskatoon, for providing *Arabidopsis NPR1/NIM1* and *TGA2* and Dr. Charles Després for useful discussions. We thank Dr. Daniel Matton for the plasmid containing the double 35S enhancer element of CaMV. D.D. was the recipient of a scholarship from the Natural Sciences and Engineering Research Council of Canada (NSERC). This work was supported by grants from NSERC to S.W.M. and N.B. and from the Fonds Concerté d'Aide à la Recherche du Québec to N.B.

Received 31 October 2000; accepted 4 June 2001

- Delaney, T.P. Genetic dissection of acquired resistance to disease. *Plant Physiol.* **113**, 5–12 (1997).
- Delaney, T.P. *et al.* A central role of salicylic acid in plant disease resistance. *Science* **266**, 1247–1250 (1994).
- Klessig, D.F. & Malamy, J. The salicylic acid signal in plants. *Plant Mol. Biol.* **26**, 1439–1458 (1994).
- Vernooij, B. *et al.* 2,6-Dichloro-isonicotinic acid-induced resistance to pathogens without the accumulation of salicylic acid. *Mol. Plant Microbe Interact.* **8**, 228–234 (1995).
- Friedrich, L. *et al.* Benzothiadiazole induces systemic acquired resistance in tobacco. *Plant J.* **10**, 61–70 (1996).
- Cao, H., Glazebrook, J., Clarke, J.D., Volko, S. & Dong, X. The *Arabidopsis NPR1* gene that controls systemic acquired resistance encodes a novel protein containing ankyrin repeats. *Cell* **88**, 57–63 (1997).
- Ryals, J.A. *et al.* The *Arabidopsis NIM1* protein shows homology to the mammalian transcription factor inhibitor I κ B. *Plant Cell* **9**, 425–439 (1997).
- Zhang, Y., Fan, W., Kinkema, M., Li, X. & Dong, X. Interaction of *NPR1* with basic leucine zipper protein transcription factors that bind sequences required for salicylic acid induction of the *PR-1* gene. *Proc. Natl. Acad. Sci. USA* **96**, 6523–6528 (1999).
- Després, C., DeLong, C., Glaze, S., Liu, E. & Fobert, P.R. The *Arabidopsis NPR1/NIM1* protein enhances the DNA binding activity of a subgroup of the TGA family of bZIP transcription factors. *Plant Cell* **12**, 279–290 (2000).
- Zhou, J.-M. *et al.* *NPR1* differentially interacts with members of the TGA/OBF family of transcription factors that bind an element of the *PR-1* gene required for induction by salicylic acid. *Mol. Plant Microbe Interact.* **13**, 191–202 (2000).
- Kinkema, M., Dan, W. & Dong, X. Nuclear localization of *NPR1* is required for activation of *PR* gene expression. *Plant Cell* **12**, 2339–2350 (2000).
- Pelletier, J.N., Campbell-Valois, F.-X. & Michnick, S.W. Oligomerization domain-directed reassembly of active dihydrofolate reductase from rationally designed fragments. *Proc. Natl. Acad. Sci. USA* **95**, 12141–12146 (1998).
- Remy, I. & Michnick, S.W. Clonal selection and *in vivo* quantification of protein interactions with protein-fragment complementation assays. *Proc. Natl. Acad. Sci. USA* **96**, 5394–5399 (1999).
- Remy, I., Wilson, I.A. & Michnick, S.W. Erythropoietin receptor activation by a ligand-induced conformation change. *Science* **283**, 990–993 (1999).
- Miyawaki, A. & Tsien, R.Y. Monitoring protein conformations and interactions by fluorescence resonance energy transfer between mutants of green fluorescent protein. *Methods Enzymol.* **327**, 472–500 (2000).
- Gadella, T.W., van der Krogt, G.N. & Bisseling, T. GFP-based FRET microscopy in living plant cells. *Trends Plant Sci.* **4**, 287–291 (1999).
- Rossi, F., Charlton, C.A. & Blau, H.M. Monitoring protein-protein interactions in intact eukaryotic cells by beta-galactosidase complementation. *Proc. Natl. Acad. Sci. USA* **94**, 8405–8410 (1997).
- Teeri, T.H. *et al.* Gene fusions to lacZ reveal new expression patterns of chimeric genes in transgenic plants. *EMBO J.* **8**, 343–350 (1989).
- Ferrell, J.E. Jr. & Machleder, E.M. The biochemical basis of an all-or-none cell fate switch in *Xenopus oocytes*. *Science* **280**, 895–898 (1998).
- Eneyedi, A.J. & Raskin, I. Induction of UDP-glucose salicylic acid glucosyltransferase activity in tobacco mosaic virus-inoculated tobacco *Nicotiana tabacum* leaves. *Plant Physiol.* **101**, 1375–1380 (1993).
- Matton, D.P., Premlott, G., Bertrand, C., Camirand, A. & Brisson, N. Identification of cis-acting elements involved in the regulation of the pathogenesis-related gene *STH-2* in potato. *Plant Mol. Biol.* **22**, 279–291 (1993).
- Delaney, T.P., Friedrich, L. & Ryals, J.A. *Arabidopsis* signal transduction mutant defective in chemically and biologically induced disease resistance. *Proc. Natl. Acad. Sci. USA* **92**, 6602–6606 (1995).
- Cao, H., Bowling, S., Gordon, A. & Dong, X. Characterization of an *Arabidopsis* mutant that is non-responsive to inducers of systemic acquired resistance. *Plant Cell* **5**, 1583–1592 (1994).
- Draper, J. Salicylate, superoxide synthesis and cell suicide in plant defence. *Trends Plant Sci.* **2**, 162–165 (1997).
- Reinold, S. & Hahlbrock, K. Biphasic temporal and spatial induction patterns of defense-related messenger RNAs and proteins in fungus-infected parsley leaves. *Plant Physiol.* **112**, 131–140 (1996).
- Remy, I. & Michnick, S.W. Visualization of biochemical networks in living cells. *Proc. Natl. Acad. Sci. USA* **98**, 7678–7683 (2001).